2-D ZO CRS stack by considering an acquisition line with smooth topography

Pedro Chira-Oliva(*), João C. R. Cruz(*), German Garabito (*), Peter Hubral(†) and Martin Tygel (‡)

(*) Federal University of Pará (Brazil), chira, jcarlos, german@ufpa.br

(†) Geophysical Institute of Karlsruhe (Germany), peter.hubral@gpi.uni-karlsruhe.de

(‡) LGC, State University of Campinas (Brazil), tygel@ime.unicamp.br

Abstract

The Common-Reflection-Surface (CRS) stack is a new method to simulate zero-offset (ZO) (stacked) sections, as well as to provide useful kinematic wavefield attributes from multi-coverage seismic data. The 2-D CRS stacking operator is based on the second-order hyperbolic traveltime approximation, which depends on three parameters. These are determined by means of an optimization process that fits the CRS stacking operator to reflection events within the multi-coverage seismic data. The objective function is semblance of the data samples along the CRS stacking operator. In this paper we present an extension of the CRS stack method that takes into account the effects of an acquisition line with smooth topography. Application to a synthetic dataset shows that the approach is able to correctly estimate the CRS parameters and produce a good stacked section in a topographic environment.

Introduction

One of the main conventional stacking methods is the Common-Midpoint (CMP) stack introduced by Mayne (1962). This method organizes the data into CMP gathers. Each CMP gather consists of source-receiver pairs symmetrically located with respect to the CMP. To stack the data along the CMP gather one uses the Normal-Moveout (NMO) correction that depends on a single parameter, the NMO velocity. In order to include effects of dip angles in the stack process, Deregowski (1986) proposed the Dip-Moveout (DMO) stack process. That method introduces a correction to the NMO procedure, however maintaining its general structure as a single parameter stack applied to the CMP gather.

As an alternative to NMO/DMO stacking process, new traveltime approaches have been introduced that are able to (a) use in the stacking procedure the full multicoverage available data (instead of CMP gathers only) and (b) perform, in an automatic way, the stacking to all time samples in the ZO section to be constructed (as opposed to the NMO method that manually chooses user-selected interpreted events and also selected CMPs for stacking). The approaches, called macro-model velocity independent methods, include the Polystack (e.g. De Bazelaire (1988)), Multifocusing (e.g. Gelchinsky et al. (1999a,b); Landa et al. (1999); Chira (2000)), and the CRS stack (e.g. Müller (1999); Mann et al. (1999); Jäger et al. (2001); Garabito (2001); Biloti (2001)). As main products, the new techniques produce high-resolution ZO sections and useful kinematic parameters. A common feature to all methods is that the subsurface model is supposed to satisfy the conditions of the zero-order ray theory. The reason of the terminology “macro-model independent methods” is that a velocity analysis, as conventionally done in the NMO method, is not required or reduced to a minimum. For a survey on the macro-velocity independent methods, the reader is referred to Hubral (1999).

As one example of a macro-model independent method, the 2-D CRS method has been introduced to simulate ZO sections from multi-coverage seismic data. 2-D means where sources and receivers are supposed to be located on a straight line (the seismic line) on the measurement surface and that the subsurface model has not much abrupt lateral variations away to the seismic line. The 2-D ZO CRS stacking operator consists of the second-order hyperbolic traveltime, that is valid for all sources and receivers that are arbitrarily located in the vicinity of a ZO point.

Land seismic data are in general affected by irregularities in the near surface, such as changes in elevation, weathering base and weathering velocity. Conventional seismic processing considers these effects as deviations from hyperbolic trends in the CMP gathers, that can be eliminated by the use of field and residual static corrections. The corrections provide generally better imaging results, but are very sensitive to the choice of parameters involved in the picking phase of the static correction. The specific case of the field static correction based on refraction seismic data suffers, for instance, from the uncertainties in the weathering velocity field.

Chira and Hubral (2003) presented the CRS operator considering the case of measurement surface (seismic line) with smooth topography. The case of a rugged topography is presented by Zhang et al. (2002). In the framework of the Multifocusing method, the case of irregular topography is considered in Gurevich et al. (2002). Chira et al. (2001) also presented an extension of the 2-D ZO CRS operator that includes, besides the smooth topography, also the effect of near-surface inhomogeneity.

According to Guo and Fagin (2002), land surveys should always be processed considering a floating datum that repre-

sents topography. They showed that velocity analysis from a flat seismic reference datum creates errors to estimate the depth and interval velocities. This problem appears even in the case of a flat topography, due to deviation of the take-off angles of the seismic ray paths.

In this paper we extend the CRS method approach presented in Garabito et al. (2001) to estimate the CRS stack parameters and produce the CRS stack, to the case of an acquisition line with smooth topography. For that, we apply the extended hyperbolic traveltime as in Chira and Hubral (2003) and Chira (2003). The CRS stack performance is examined by means of its application of a synthetic seismic dataset.

Theory

The 2-D CRS stacking operator depends on three parameters that are associated with two hypothetical waves, namely the normal-incidence-point (NIP) and Normal (N) waves (Hubral, 1983). The parameters are the emergence angle of the normal ray, and two wavefront curvatures. The emergence point, X_0, of the normal ray is called central point. The NIP wave propagates upwards from a point source located at the normal ray incidence point. On the other hand, the N wave propagates upwards starting as a wavefront that coincides with reflector in the vicinity of the NIP.

The CRS stack traveltime approximation with smooth topography and without considering near-surface inhomogeneity effects (i.e., gradients) in the vicinity of the central point, is given in Chira et al. (2001),

$$t^2(x_m,h) = \left(t_0 + 2\,\frac{\sin\beta_0{}^*}{v_1}\,(x_m - x_0)\right)^2 + \frac{2\,t_0}{v_1}\left(\frac{\cos^2\beta_0^*}{R_N} - \cos\beta_0^*\,K_0\right)(x_m - x_0)^2 + \frac{2\,t_0}{v_1}\left(\frac{\cos^2\beta_0^*}{R_{NIP}} - \cos\beta_0^*\,K_0\right)h^2\,. \tag{1}$$

Here, t_0 and x_0 are the ZO reflection traveltime and the central point coordinate, respectively and v_1 is the near-surface velocity of the P-P wave at the central point. Also, x_m and h are, respectively, the midpoint and half-offset coordinates on the x_1-axis, that is tangent to the curved surface with origin at the central point X_0 (see Figures 1a,b). β_0^* is the emergence angle of the normal ray at the topographic surface at the central point. The parameter K_0 is the local curvature of the acquisition line, taken as positive if this line falls below its tangent at X_0 and negative if it falls above this tangent. R_{NIP} and R_N are the radii of curvatures of the emerging hypothetical NIP and N wavefronts at X_0, respectively. The parameters R_{NIP}, R_N and β_0^* are to be automatically derived from the multi-coverage seismic data.

In order to regularize the processing coordinates, we apply a transformation from the local Cartesian system (x_1, x_3) into the global Cartesian system (x, z) of Figure 1b. The midpoint and half-offset coordinates, (x_m, h) and (x'_m, h'),

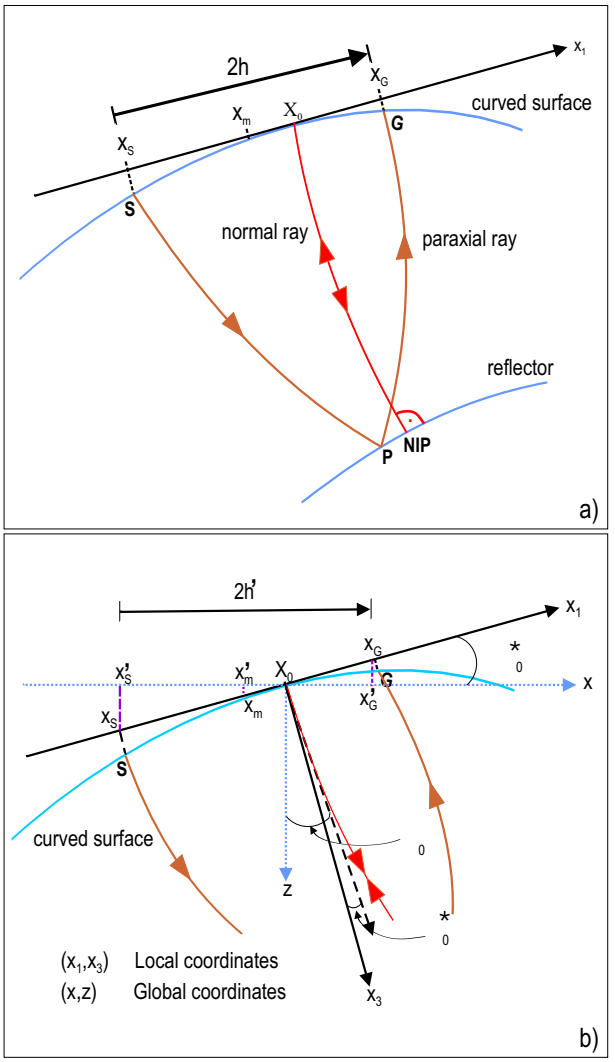

Figure 1: a)Ray diagram for a paraxial ray in the vicinity of a normal ray in a 2-D laterally inhomogeneous medium. Definition of local coordinates of a paraxial SPG for a curved measurement surface with respect to point X_0. b)Transformation of the local coordinates, x_m and h, to its global coordinates $x_m{}'$ and h'. α_0^* is the local dip angle of the tangent at X_0 (x_1-axis). β_0 is the angle between the normal ray and the vertical line through X_0 (z-axis) and β_0^* is the angle between the normal ray and the normal to the tangent at X_0.

in the local and global coordinate systems, respectively, are related by the expressions

$$h = \frac{h'}{\cos\alpha_0^*}\ , \quad x_m = \frac{x'_m}{\cos\alpha_0^*}\ , \tag{2}$$

where α_0^* is the dip angle of the tangent x_1-axis at point X_0. Introducing the relationships (2) into equation (1), we find (Chira and Hubral, 2003)

$$\begin{aligned} t^2_{dif}(x'_m, h') = & \left(t_0 + 2\ \frac{\sin\beta_0{}^*}{v_1\cos\alpha_0^*}\ (x'_m - x_0)\right)^2 \\ & + \frac{2\ t_0}{v_1\cos^2\alpha_0^*}\left(\frac{\cos^2\beta_0^*}{R_N} - \cos\beta_0^*\ K_0\right)(x'_m - x_0)^2 \\ & + \frac{2\ t_0}{v_1\cos^2\alpha_0^*}\left(\frac{\cos^2\beta_0^*}{R_{NIP}} - \cos\beta_0^*\ K_0\right)(h')^2\ . \end{aligned} \tag{3}$$

We now consider a *pure diffraction*, i.e., the situation in which the reflector reduces to a single diffraction point. In this case, the NIP and N waves are coincident, that is, both propagate from a point source at NIP and have identical radii of curvatures at X_0, i.e. $R_N \equiv R_{NIP}$. As a consequence, equation (3) becomes

$$\begin{aligned} t^2(x'_m, h') = & \left(t_0 + 2\ \frac{\sin\beta_0{}^*}{v_1\ \cos\alpha_0^*}\ (x'_m - x_0)\right)^2 \\ & + \frac{2\ t_0}{v_1\cos^2\alpha_0^*}\left(\frac{\cos^2\beta_0^*}{R_{NIP}} - \cos\beta_0^*\ K_0\right)\left((x'_m - x_0)^2 + (h')^2\right)\ . \end{aligned} \tag{4}$$

Equation (4) depends on two CRS parameters (R_{NIP}, β_0^*) associated to the NIP wave. This equation will be used in the first step of the CRS strategy shown below. The CRS stacking operator defined by equation (4) is an approximation of the pre-stack Kirchhoff migration operator with smooth topography.

Setting the condition $h' = 0$ to the general hyperbolic traveltime equation (3), the CRS stacking operator for reflected (and diffracted) events in the ZO configuration. We have,

$$\begin{aligned} t^2_{ZO}(x'_m) = & \left(t_0 + 2\ \frac{\sin\beta_0{}^*}{v_1\ \cos\alpha_0^*}\ (x'_m - x_0)\right)^2 \\ & + \frac{2\ t_0}{v_1\cos^2\alpha_0^*}\ \left(\frac{\cos^2\beta_0^*}{R_N} - \cos\beta_0^*\ K_0\right)\ (x'_m - x_0)^2\ . \end{aligned} \tag{5}$$

Equation (5), that depends on the two CRS parameters (R_N, β_0^*), is the one that will be used in the second step of CRS strategy shown below .

2-D ZO CRS stack

In the 2-D situation considered here, for each point $P_0(x_0, t_0)$ at the ZO section to be simulated, the amplitudes in the seismic data will be summed (stacked) along the moveout curve defined by equation (3). The resulting (stacked) amplitude is assigned to the given point P_0.

The three CRS stacking parameters $(\beta_0^*, R_{NIP}, R_N)$ are estimated by means of an optimization process, having the semblance as objective function. The CRS stacking optimization problem consists of estimating the parameters that maximize the semblance. In general, the problem requires a combination of multi-dimensional global and local optimization algorithms. The mathematical intervals defined for the parameters are $-\pi/2 < \beta_0^* < \pi/2$, $-\infty < R_{NIP}, R_N < \infty$. Optimization strategies to estimate these parameters are found in the literature (e.g. Müller (1999); Birgin et al. (1999); Garabito et al. (2001)).

In this paper, we apply the strategy given by Garabito et al. (2001) to estimate the CRS parameters triplet, but using the new equations (3), (4) and (5).

CRS stack processing strategy

The proposed strategy to carry out the CRS method involves a combination of global and local search processes and is divided into three steps. The curvature, K_0, of the seismic line at each central point is supposed to be a priori known or calculated by means of some interpolation method. At the first and second steps we used the Simulated Annealing (SA) algorithm (Sen and Stoffa, 1995), and at the third step the Variable Metric (VM) algorithm (Bard (1974); Gill et al. (1981)). Each step is performed on each given sample point $P_0(x_0, t_0)$ that pertains to the ZO section to be simulated.

Step I : Pre-Stack Global Optimization The multi-coverage pre-stack seismic data is the input. The inverse problem consists of simultaneously estimating the two parameters β_0^* and R_{NIP} that provide the maximum semblance value, according equation (4). The results of this step are: 1) maximum coherence section, 2) emergence angle, β_0^*- section, 3)NIP-wave radius of curvature, R_{NIP}-section, and 4)simulated (stacked) ZO section.

Step II : Post-Stack Global Optimization The post-stack seismic data is the input. The inverse problem consists of estimating the single parameter, R_N, that provides the maximum semblance according to equation (5), in which the previously obtained parameter, β_0^*, is kept fixed. In this step the results are: 1) maximum coherence section, 2)N-wave radius of curvature, R_N-section, and 3)re-stacked simulated ZO (stacked) section.

Step III : Pre-Stack Global Optimization The multi-coverage pre-stack seismic data is the input. The inverse problem consists of estimating the best parameter triplet $(\beta_0^*, R_{NIP}, R_N)$ that provides the maximum semblance. In this case the CRS stacking operator is equation (3), applied to the full multi-coverage dataset with suitable apertures. In this step the results are: 1) maximum coherence section, 2) optimized β_0^*-section, 3)optimized R_{NIP}-section, 4)optimized R_N-section, and 5)optimized ZO (stacked) section.

Example

In order to test the CRS stacking algorithm we consider its application to a synthetic dataset computed for the 2-D homogeneous layered model shown in Figure 2. The model consists of four layers above a half-space. The acquisition line presents a smooth topography. On this model, we generate a synthetic dataset of multi-coverage primary reflections, using the ray-tracing algorithm, SEIS88

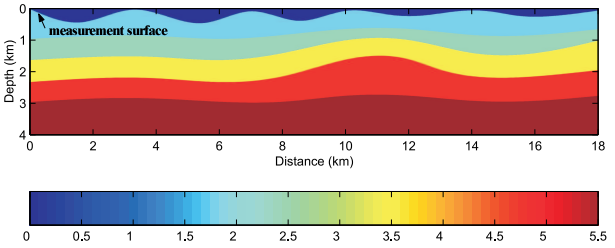

Figure 2: 2-D model constituted of five isovelocity layers with curved interfaces and curved measurement surface. Interval velocities are 1.75 km/s, 2.4 km/s, 3.5 km/s, 4.65 km/s and 5.5 km/s, respectively.

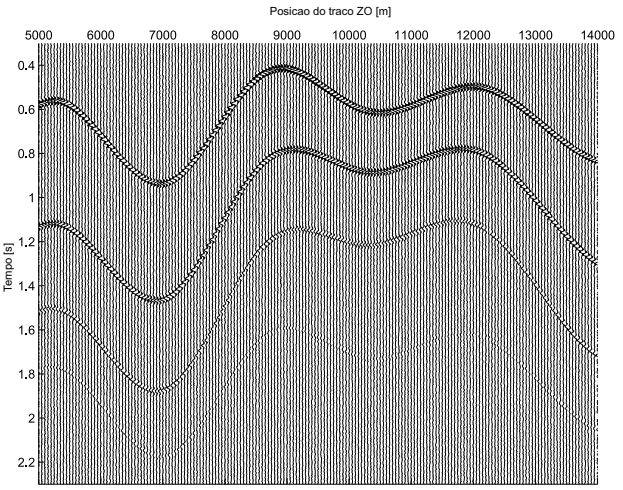

Figure 3: ZO section with random noise (ratio S/N = 10) obtained by forward modelling.

(Červený and Pšěnsik, 1988). It was added random noise with signal-to-noise ratio of $S/N = 10$. The dataset consists of 201 common-shots (CS) with 72 geophones with separation interval of 50 meters. The minimum offset is 50 meters. The source signal is a Gabor wavelet with 40 Hz dominant frequency and the time sampling is 4 ms.

Figure 3 shows the ray-theoretical modelled ZO section. Next, Figure 4 shows the simulated ZO section that results from the application of the CRS stacking method for a curved measurement surface. Due to the fact that the CRS method involves a larger number of traces during the stacking process, the simulated ZO section presents enhanced primary reflection events, with larger signal-to-noise ratio than the corresponding ones in the modelled ZO section (Figure 3). Figure 5 shows the maximum coherence (semblance) section that corresponds to the optimized parameters. We note that the coherence values become smaller for larger traveltimes (deeper events). Figures 6, 7 and 8 show the sections of emergence angle and radii of curvature of the NIP and N waves, respectively. These sections correspond to optimized global maxima determined in the third step.

A comparison between the emergence angles, β_0^*, estimated by the CRS algorithm and by modelling, respectively, is shown in Figure 9. We can see that the angle parameter has been well estimated along all reflectors. Figures 10 and 11 show the analogous comparison for the other parameters, R_{NIP} e R_N, respectively. These parameters are also well estimated, with the exception of the locations where abrupt changes of the topography are present.

Conclusions

A new formula for the CRS stacking method that considers the curvature of the acquisition line has been tested in synthetic data sets with successful results. The parameters were correctly estimated, except in the regions where there are abrupt changes of the topography. In these regions, the inaccuracies of the estimated parameters increases with depth.

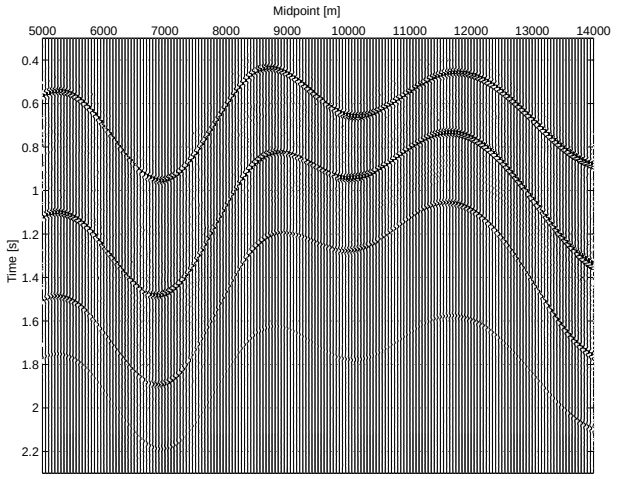

Figure 4: Simulated ZO section with the ZO CRS stack by using the multi-coverage seismic data with random noise (ratio S/N = 10).

Acknowledgements

We thank the financial support in part by the Project “Imageamento sísmico em bacias paleózoicas com soleiras de diabásio na região Amazônica (IMAGAM)” of CT-PETRO/FINEP/CNPq/UFPA. The first author also thanks to the National Council of Technology and Development (CNPq), Brazil, for the scholarship, and to the sponsors of the Wave Inversion Technology (WIT) Consortium (Germany) for their support.

References

Bard, B., 1974, Nonlinear parameter estimation: Academic Press.

Biloti, R., 2001, Tempo de Trânsito Multiparamétricos: Estimação e Inversão (in portuguese): Ph.D. thesis, State University of Campinas (Brazil).

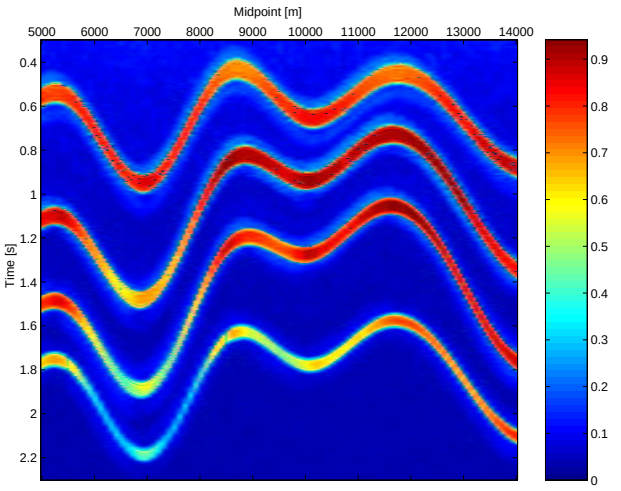

Figure 5: CRS optimized coherence section of the model of Figure 2.

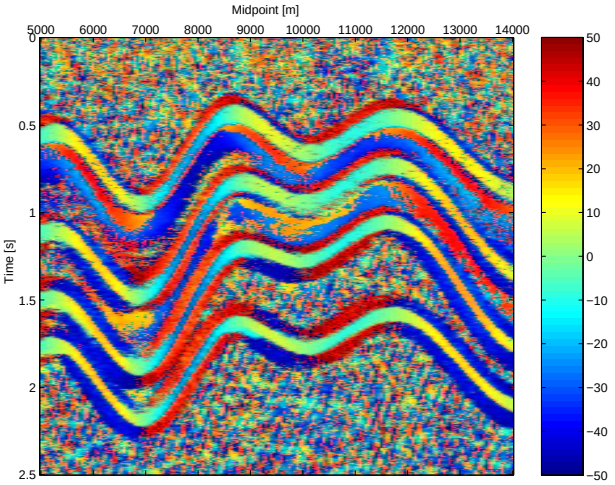

Figure 6: CRS optimized β_0^*-section of the model of Figure 2.

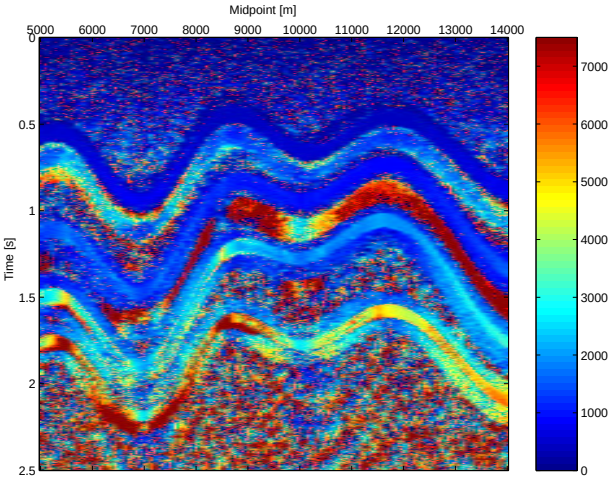

Figure 7: CRS optimized R_{NIP}-section of the model of Figure 2.

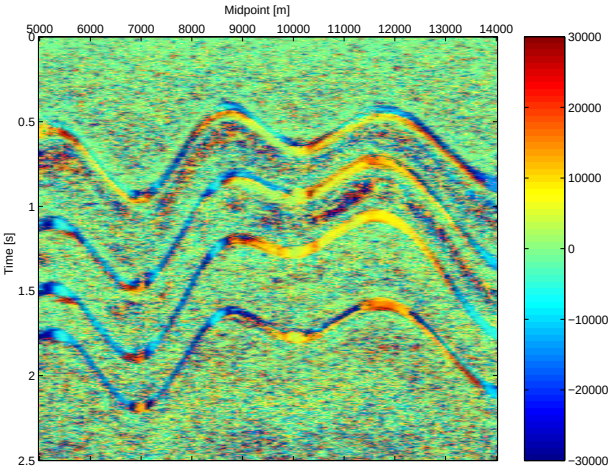

Figure 8: CRS optimized R_N-section of the model of Figure 2.

Birgin, E. G., Biloti, R., Tygel, M., and Santos, T. L., 1999, Restricted optimization: a clue to a fast and accurate implementation of the Common Reflection Surface Stack method: J. Appl. Geoph., **42**, no. 3,4, 143–155.

Chira, P., and Hubral, P., 2003, Traveltime formulas of near-zero-offset primary reflections for a curved 2-D measurement surface: Geophysics, **68**, no. 1, 255–261.

Chira, P., Tygel, M., Zhang, Y., and Hubral, P., 2001, Analytic CRS Stack formula for a 2D curved measurement surface and finite-offset reflections: Journal of Seismic Exploration, **5**, no. 10, 245–262.

Chira, P., 2000, Imageamento Multifoco de Refletores Sísmicos (in protuguese): Master's thesis, Federal University of Para (Brazil).

Chira, P., 2003, Empilhamento pelo método Superfície de Reflexão Comum 2-D com Topografia e Introdução ao caso 3-D (in portuguese): Ph.D. thesis, Federal University of Para (Brazil).

De Bazelaire, E., 1988, Normal moveout revisited - inhomogeneous media and curved interfaces: Geophysics, **53**, no. 2, 143–157.

Deregowski, S. M., 1986, What is DMO?: First Break, **4**, no. 7, 7–24.

Garabito, G., Cruz, J. C. R., Hubral, P., and Costa, J., 2001, Common reflection surface stack by global optimization: 71th Annual Internat. Mtg., Soc. Expl. Geophys., Expanded Abstracts.

Garabito, G., 2001, Empilhamento Sísmico por Superfície de Reflexão Comum: um novo algoritmo usando Otimização Global e Local (in portuguese): Ph.D. thesis, Federal University of Para (Brazil).

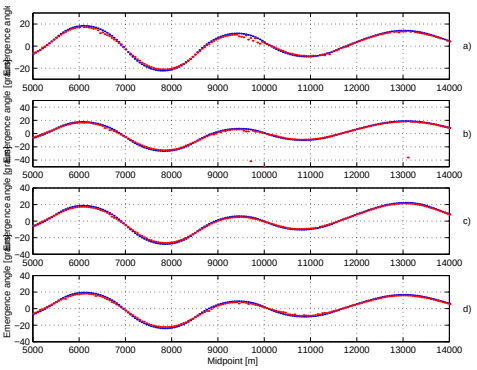

Figure 9: Comparison between CRS (red points) and model-derived (blue points) emergence angles β_0^*. The parameter for each interface are plotted separately: a) first, b) second, c) third and d) fourth interface of the model of Figure 2.

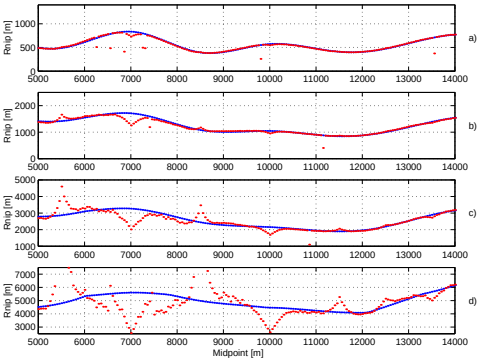

Figure 10: Comparison between CRS (red points) and model-derived (blue points) radius of curvature, R_{NIP}. The parameter for each interface are plotted separately: a) first, b) second, c) third and d) fourth interface of the model of Figure 2.

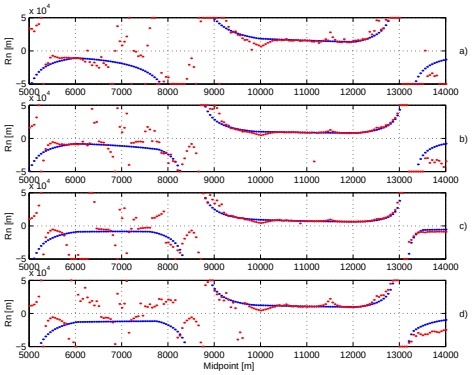

Figure 11: Comparison between CRS (red points) and model-derived (blue points) radius of curvature, R_N. The parameter for each interface are plotted separately: a) first, b) second, c) third and d) fourth interface of the model of Figure 2.

Gelchinsky, B., Berkovitch, A., and Keydar, S., 1999a, Multifocusing homeomorphic imaging. Part I. Basic concepts and formulas. Special Issue: Macro-Model Independent Seismic Reflection Imaging: J. Appl. Geoph., **42**, no. 3,4, 229–242.

——— 1999b, Multifocusing homeomorphic imaging. Part II. Multifold data set and Multifocusing. Special Issue: Macro-Model Independent Seismic Reflection Imaging: J. Appl. Geoph., **42**, no. 3,4, 243–260.

Gill, P. E., Murray, W., and Wright, M. H., 1981, Practical optimization: Academic Press.

Guo, N., and Fagin, S., 2002, Becoming effective velocity-model builders and depth imagers, part 2 - the basics of velocity-model building, examples and discussions: The Leading Edge, pages 1210–1216.

Gurevich, B., Keydar, S., and Landa, E., 2002, Multifocusing imaging over an irregular topography: Geophysics, **67**, 639–643.

Hubral, P., 1983, Computing true amplitude reflections in a laterally inhomogeneous earth: Geophysics, **48**, no. 8, 1051–1062.

Hubral, P., 1999, Macro-model independent seismic reflection imaging: J. Appl. Geoph., **42**, no. 3,4.

Jäger, R., Mann, J., Höcht, G., and Hubral, P., 2001, Common-reflection-surface stack: Image and attributes: Geophysics, **66**, no. 1, 97–109.

Landa, E., Gurevich, B., Keydar, S., and Trachman, P., 1999, Multifocusing Stack - a New Time Imaging Method: 6th Annual Congress, SBGf, Expanded Abstracts, 195.

Mann, J., Jäger, R., Müller, T., Höcht, G., and Hubral, P., 1999, Common-reflection-surface stack - a real data example: J. Appl. Geoph., **42**, no. 3,4, 301–318.

Mayne, W. H., 1962, Common reflection point horizontal data stacking techniques: Geophysics, **27**, no. 6, 927–938.

Müller, T., 1999, The common reflection surface stack - seismic imaging without explicit knowledge of the velocity model: Der Andere Verlag, Bad Iburg.

Sen, M., and Stoffa, L. P., 1995, Global optimization methods in geophysical inversion: Netherlands, Elsevier Science.

Červený, V., and Pšěnsik, I., 1988, Ray tracing program package: .

Zhang, Y., Höcht, G., and Hubral, P., 2002, 2D and 3D ZO CRS stack for a complex top-surface topography: 64th Annual Internat. Mtg., Eur. Assoc. Expl. Geophys., Extended Abstracts.